A guide to choosing fluorescent proteins

Nathan C Shaner[1,2], Paul A Steinbach[1,3] & Roger Y Tsien[1,3,4]

The recent explosion in the diversity of available fluorescent proteins (FPs)[1–16] promises a wide variety of new tools for biological imaging. With no unified standard for assessing these tools, however, a researcher is faced with difficult questions. Which FPs are best for general use? Which are the brightest? What additional factors determine which are best for a given experiment? Although in many cases, a trial-and-error approach may still be necessary in determining the answers to these questions, a unified characterization of the best available FPs provides a useful guide in narrowing down the options.

We can begin by stating several general requirements for the successful use of an FP in an imaging experiment. First, the FP should express efficiently and without toxicity in the chosen system, and it should be bright enough to provide sufficient signal above autofluorescence to be reliably detected and imaged. Second, the FP should have sufficient photostability to be imaged for the duration of the experiment. Third, if the FP is to be expressed as a fusion to another protein of interest, then the FP should not oligomerize. Fourth, the FP should be insensitive to environmental effects that could confound quantitative interpretation of experimental results. Finally, in multiple-labeling experiments, the set of FPs used should have minimal crosstalk in their excitation and emission channels. For more complex imaging experiments, such as those using fluorescence resonance energy transfer (FRET)[17] or selective optical labeling using photoconvertible FPs[12,15], additional considerations come into play. General recommendations to help determine the optimal set of FPs in each spectral class for a given experiment are available in Box 1, along with more detail on each issue discussed below.

'Brightness' and expression

FP vendors typically make optimistic but vague claims as to the brightness of the proteins they promote. Purely qualitative brightness comparisons that do not provide clear information on the extinction coefficient and quantum yield should be viewed with skepticism.

For example, the newly released DsRed-Monomer (Clontech) is described as "bright," even though in fact, it is the dimmest monomeric red fluorescent protein (RFP) presently available.

The perceived brightness of an FP is determined by several highly variable factors, including the intrinsic brightness of the protein (determined by its maturation speed and efficiency, extinction coefficient, quantum yield and, in longer experiments, photostability), the optical properties of the imaging setup (illumination wavelength and intensity, spectra of filters and dichroic mirrors), and camera or human eye sensitivity to the emission spectrum. Although these factors make it impossible to name any one FP as the brightest overall, it is possible to identify the brightest protein in each spectral class (when more than one protein is available), as this depends only on the intrinsic optical properties of the FP. The brightest proteins for each class are listed in Table 1, with greater detail on the properties of each listed protein available in Supplementary Table 1 online. As discussed below in relation to photostability, the choice of optimal filter sets is critical to obtaining the best performance from an FP.

Generally, FPs that have been optimized for mammalian cells will express well at 37 C, but some proteins may fold more or less efficiently. We have not done extensive tests in mammalian cells to determine relative efficiency of folding and maturation at 37 C versus lower temperatures, but expression of proteins in

[1]Department of Pharmacology, [2]Biomedical Sciences Graduate Program, [3]Howard Hughes Medical Institute and [4]Department of Chemistry and Biochemistry, 310 Cellular & Molecular Medicine West 0647, University of California at San Diego, 9500 Gilman Drive, La Jolla, CA 92093, USA. Correspondence should be addressed to R.Y.T. (rtsien@ucsd.edu).

bacteria at 37 C versus 25 C gives some indication of the relative efficiencies. These experiments suggest that there are several proteins that do not mature well at 37 C. Indications of potential folding inefficiency at 37 C should not be taken with absolute certainty, however, as additional chaperones and other differences between mammalian cells and bacteria (and even variations between mammalian cell lines) could have substantial influences on folding and maturation efficiency.

Generally, modern *Aequorea*-derived fluorescent proteins (AFPs, see **Supplementary Table 2** online for mutations of common AFP variants relative to wild-type GFP) fold reasonably well at 37 C—in fact, several recent variants have been specifically optimized for 37 C expression. The UV-excitable variant T-Sapphire[6] and the yellow AFP (YFP) variant Venus[1] are examples of these. The best green GFP variant, Emerald[18], also folds very efficiently at 37 C compared with its predecessor, enhanced GFP (EGFP). The only recently developed AFP that performed poorly in our tests was the cyan variant, CyPet[2], which folded well at room temperature but poorly at 37 C. All orange, red and far-red FPs (with the exception of J-Red and DsRed-Monomer) listed in Table 1 perform well at 37 C.

An additional factor affecting the maturation of FPs expressed in living organisms is the presence or absence of molecular oxygen. The requirement for O_2 to dehydrogenate amino acids during chromophore formation has two important consequences. First, each molecule of AFP should generate one molecule of H_2O_2 as part of its maturation process[18], and the longer-wavelength FPs from corals probably generate two[19]. Second, fluorescence formation is prevented by rigorously anoxic conditions (< 0.75 M O_2), but is readily detected at 3 M O_2 (ref. 20). Even when anoxia initially prevents fluorophore maturation, fluorescence measurements are usually done after the samples have been exposed to air[21].

Photostability

All FPs eventually photobleach upon extended excitation, though at a much lower rate than many small-molecule dyes (Table 1). In addition, there is substantial variation in the rate of photobleaching between different FPs—even between FPs with otherwise very similar optical properties. For experiments requiring a limited number of images (around 10 or fewer), photostability is generally not a major factor, but choosing the most photostable protein is critical to success in experiments requiring large numbers of images of the same cell or field.

A unified characterization of FP photostability has until now been lacking in the scientific literature. Although many descriptions of new FP variants include some characterization of their photostability, the methods used for this characterization are highly variable and the resulting data are impossible to compare directly. Because many FPs have complex photobleaching curves and require different excitation intensities and exposure times, a standardized treatment of photostability must take all these factors into account.

To provide a basis for comparing the practical photostability of FPs, we have measured photobleaching curves for all of the FPs listed in Table 1 under conditions designed to effectively simulate wide-field microscopy of live cells[4]. Briefly, aqueous droplets of purified FPs (at pH 7) were formed under mineral oil in a chamber that allows imaging on a fluorescence microscope. Droplets of volumes comparable to those of typical mammalian cells were photobleached with continuous illumination while recording images periodically to generate a bleaching curve. To account for differences in brightness between proteins and efficiency of excitation in our microscope setup, we normalized each bleaching curve to account for the extinction coefficient and quantum yield of the FP, the emission spectrum of the arc lamp used for excitation, and the transmission spectra of the filters and other optical path components of the microscope

BOX 1 RECOMMENDATIONS BY SPECTRAL CLASS

Far-red. mPlum is the only reasonably bright and photostable far-red monomer available. Although it is not as bright as many shorter-wavelength options, it should be used when spectral separation from other FPs is critical, and it may give some advantage when imaging thicker tissues. AQ143, a mutated anemone chromoprotein, has comparable brightness ($\varepsilon = 90$ (mM • cm)$^{-1}$, quantum yield (QY) = 0.04) and even longer wavelengths (excitation, 595 nm; emission, 655 nm), but it is still tetrameric[31].

Red. mCherry is the best general-purpose red monomer owing to its superior photostability. Its predecessor mRFP1 is now obsolete. The tandem dimer tdTomato is equally photostable but twice the molecular weight of mCherry, and may be used when fusion tag size does not interfere with protein function. mStrawberry is the brightest red monomer, but it is less photostable than mCherry, and should be avoided when photostability is critical. We do not recommend using J-Red and DsRed-Monomer.

Orange. mOrange is the brightest orange monomer, but should not be used when photostability is critical or when it is targeted to regions of low or unstable pH. mKO is extremely photostable and should be used for long-term or intensive imaging experiments or when targeting to an acidic or pH-unstable environment.

Yellow-green. The widely used variant EYFP is obsolete and inferior to mCitrine, Venus and YPet. Each of these should perform well in most applications. YPet should be used in conjunction with the CFP variant CyPet for FRET applications.

Green. Although it has a more pronounced fast bleaching component than the common variant EGFP, the newer variant Emerald exhibits far more efficient folding at 37 C and will generally perform much better than EGFP.

Cyan. Cerulean is the brightest CFP variant and folds most efficiently at 37 C, and thus, it is probably the best general-purpose CFP. Its photostability under arc-lamp illumination, however, is much lower than that of other CFP variants. CyPet appears superior to mCFP in that it has a somewhat more blue-shifted and narrower emission peak, and displays efficient FRET with YFP variant YPet, but it expresses relatively poorly at 37 C.

UV-excitable green. T-Sapphire is potentially useful as a FRET donor to orange or red monomers.

(see[4] and Supplementary Discussion online for additional description of bleaching calculations). This method of normalization provides a practical measurement of how long each FP will take to lose 50% of an initial emission rate of 1,000 photons/s. Because dimmer proteins will require either higher excitation power or longer exposures, we believe this method of normalization provides a realistic picture of how different FPs will perform in an actual experiment imaging populations of FP molecules. Bleaching experiments were performed in parallel for several (but not all) of the FPs listed in Table 1 expressed in live cells and gave time courses closely matching those of purified proteins in microdroplets.

Based on our photobleaching assay results, it is clear that photostability can be highly variable between different FPs, even those of the same spectral class. Taking into account brightness and folding efficiencies at 37 C, the best proteins for long-term imaging are the monomers mCherry and mKO. The red tandem dimer tdTomato is also highly photostable and may be used when the size of the fusion tag is not of great concern. The relative photostability of proteins in each spectral class is indicated in Table 1. Some AFPs, such as Cerulean, had illumination intensity–dependent fast bleaching components, and so photobleaching curves were taken at lower illumination intensities where this effect was less pronounced. The GFP variant Emerald displayed a very fast initial bleaching component that led to an extremely short time to 50% bleach. But after this initial fast bleaching phase, its photostability decayed at a rate very similar to that of EGFP. All YFPs, with the exception of Venus, have reasonably good photostability, and thus, YFP selection should be guided by brightness, environmental sensitivity or FRET performance (see Box 1 for greater detail and for general recommendations for all spectral classes, and Supplementary Fig. 1 online for sample bleaching curves).

Our method of measuring photobleaching has some limitations in its applicability to different imaging modalities, such as laser scanning confocal microscopy. Although we believe that our measurements are valid for excitation light intensities typical of standard epifluorescence microscopes with arc lamp illumination (up to 10 W/cm^2), higher intensity (for example, laser) illumination (typically >>100 W/cm^2) evokes nonlinear effects that we cannot predict with our assay. For example, we have preliminary indications that even though the first monomeric red FP, mRFP1, shows approximately tenfold faster photobleaching than the second-generation monomer mCherry, both appear to have similar bleaching times when excited at 568 nm on a laser scanning confocal microscope. The CFP variant Cerulean appears more photostable than ECFP with laser illumination on a confocal microscope[3] but appears less photostable than ECFP with arc lamp illumination. Such inconsistencies between bleaching behavior at moderate versus very high excitation intensities are likely to occur with many FPs. Single-molecule measurements will be even less predictable based on our population measurements, because our extinction coefficients are averages that include poorly folded or nonfluorescent molecules, whereas single-molecule observations exclude such defective molecules.

It is critical to choose filter sets wisely for experiments that require long-term or intensive imaging. Choosing suboptimal filter sets will lead to markedly reduced apparent photostability owing to the need to use longer exposure times or greater illumination intensities to obtain sufficient emission intensity.

Table 1 | Properties of the best FP variants[a,b]

Class	Protein	Source laboratory (references)	Excitation[c] (nm)	Emission[d] (nm)	Brightness[e]	Photostability[f]	pKa	Oligomerization
Far-red	mPlum[g]	Tsien (5)	590	649	4.1	53	<4.5	Monomer
Red	mCherry[g]	Tsien (4)	587	610	16	96	<4.5	Monomer
	tdTomato[g]	Tsien (4)	554	581	95	98	4.7	Tandem dimer
	mStrawberry[g]	Tsien (4)	574	596	26	15	<4.5	Monomer
	J-Red[h]	Evrogen	584	610	8.8*	13	5.0	Dimer
	DsRed-monomer[h]	Clontech	556	586	3.5	16	4.5	Monomer
Orange	mOrange[g]	Tsien (4)	548	562	49	9.0	6.5	Monomer
	mKO	MBL Intl. (10)	548	559	31*	122	5.0	Monomer
Yellow-green	mCitrine[i]	Tsien (16,23)	516	529	59	49	5.7	Monomer
	Venus	Miyawaki (1)	515	528	53*	15	6.0	Weak dimer[j]
	YPet[g]	Daugherty (2)	517	530	80*	49	5.6	Weak dimer[j]
	EYFP	Invitrogen (18)	514	527	51	60	6.9	Weak dimer[j]
Green	Emerald[g]	Invitrogen (18)	487	509	39	0.69[k]	6.0	Weak dimer[j]
	EGFP	Clontech[l]	488	507	34	174	6.0	Weak dimer[j]
Cyan	CyPet	Daugherty (2)	435	477	18*	59	5.0	Weak dimer[j]
	mCFPm[m]	Tsien (23)	433	475	13	64	4.7	Monomer
	Cerulean[g]	Piston (3)	433	475	27*	36	4.7	Weak dimer[j]
UV-excitable green	T-Sapphire[g]	Griesbeck (6)	399	511	26*	25	4.9	Weak dimer[j]

[a]An expanded version of this table, including a list of other commercially available FPs, is available as **Supplementary Table 1**. [b]The mutations of all common AFPs relative to the wild-type protein are available in **Supplementary Table 3**. [c]Major excitation peak. [d]Major emission peak. [e]Product of extinction coefficient and quantum yield at pH 7.4 measured or confirmed (indicated by *) in our laboratory under ideal maturation conditions, in (mM • cm)−1 (for comparison, free fluorescein at pH 7.4 has a brightness of about 69 (mM • cm)−1). [f]Time for bleaching from an initial emission rate of 1,000 photons/s down to 500 photons/s ($t_{1/2}$; for comparison, fluorescein at pH 8.4 has $t_{1/2}$ of 5.2 s); data are not indicative of photostability under focused laser illumination. [g]Brightest in spectral class. [h]Not recommended (dim with poor folding at 37 °C). [i]Citrine YFP with A206K mutation; spectroscopic properties equivalent to Citrine. [j]Can be made monomeric with A206K mutation. [k]Emerald has a pronounced fast bleaching component that leads to a very short time to 50% bleach. Its photostability after the initial few seconds, however, is comparable to that of EGFP. [l]Formerly sold by Clontech, no longer commercially available. [m]mECFP with A206K mutation; spectroscopic properties equivalent to ECFP.

Oligomerization and toxicity

Unlike weakly dimeric AFPs, most newly discovered wild-type FPs are tightly dimeric or tetrameric[7,9–12,14,22]. Many of these wild-type proteins, however, can be engineered into monomers or tandem dimers (functionally monomeric though twice the molecular weight), which can then undergo further optimization[4,10,12,17]. Thus, even though oligomerization caused substantial trouble in the earlier days of red fluorescent proteins (RFPs), there are now highly optimized monomers or tandem dimers available in every spectral class. Although most AFPs are in fact very weak dimers, they can be made truly monomeric simply by introducing the mutation A206K, generally without deleterious effects[23]. Thus, any of the recommended proteins in Table 1 should be capable of performing well in any application requiring a monomeric fusion tag. Researchers should remain vigilant of this issue, however, and always verify the oligomerization status of any new or 'improved' FPs that are released. Lack of visible precipitates does not rule out oligomerization at the molecular level.

It is rare for FPs to have obvious toxic effects in most cells in culture, but care should always be taken to do the appropriate controls when exploring new cell lines or tissues. As so many new FPs have become available, it is unknown whether any may be substantially more toxic to cells than AFPs. In our hands, tetrameric proteins can be somewhat toxic to bacteria, especially if they display a substantial amount of aggregation, but monomeric proteins are generally nontoxic. It seems difficult or impossible to generate transgenic mice widely expressing tetrameric RFPs, whereas several groups have successfully obtained mice expressing monomeric RFPs[24,25].

Environmental sensitivity

When images must be quantitatively interpreted, it is critical that the fluorescence intensity of the protein used not be sensitive to factors other than those being studied. Early YFP variants were relatively chloride sensitive, a problem that has been solved in the Citrine and Venus (and likely YPet) variants[1,2,16]. Most FPs also have some acid sensitivity. For general imaging experiments, all FPs listed in Table 1 have sufficient acid resistance to perform reliably. More acid-sensitive FPs, however, may give poor results when targeted to acidic compartments such as the lumen of lysosomes or secretory granules, and may confound quantitative image interpretation if a given stimulus or condition leads to altered intracellular pH. Because of this, one should avoid using mOrange[4], GFPs or YFPs for experiments in which acid quenching could produce artifacts. Conversely, the pH sensitivity of these proteins can be very valuable to monitor organellar luminal pH or exocytosis[26,27].

Multiple labeling

One of the most attractive prospects presented by the recent development of such a wide variety of monomeric FPs is for multiple labeling of fusion proteins in single cells. Although linear unmixing systems promise the ability to distinguish between large numbers of different fluorophores with partially overlapping spectra[28], it is possible even with a simpler optical setup to clearly distinguish between three or four different FPs. Using the filter sets recommended in Table 2, one may image cyan, yellow, orange and red (Cerulean or CyPet, any YFP, mOrange or mKO and mCherry) simultaneously with minimal crosstalk. To produce even cleaner spectral separation, one could image cyan, orange and far-red (Cerulean or CyPet, mOrange or mKO, and mPlum)[2,4,5,10].

Additional concerns for complex experiments

For more complex imaging experiments, additional factors come into play when choosing the best genetically encoded fluorescent probe, many of which are beyond the scope of this perspective. For FRET applications, the choice of appropriate donor and acceptor FPs may be critical, and seemingly small factors (such as linker length and composition for intramolecular FRET constructs) may have a substantial role. The recent development of the FRET-optimized cyan-yellow pair CyPet and YPet holds great promise for the improvement of FRET sensitivity[2], and it is the current favorite as a starting point for new FRET sensors but has yet to be proven in a wide variety of constructs. For experiments requiring photoactivatable or photoconvertible tags, several options are available, including photoactivatable GFP (PA-GFP)[15] and monomeric RFP (PA-mRFP)[13], reversibly photoswitchable Dronpa[29], the tetrameric kindling fluorescent protein (KFP)[9], and the green-to-red photoconvertible proteins KikGR[14] and EosFP[12] (the latter is available as a bright tandem dimer) and cyan-to-green photoconvertible monomer PS-CFP[8]. A more detailed (but probably not exhaustive) list of options for these more advanced applications of FPs are listed in Supplementary Table 3 online. In addition, a recent review is available detailing the potential applications of photoactivatable FPs[30].

Future developments

Although the present set of FPs has given researchers an unprecedented variety of high-performance options, there are still many areas that could stand improvement. In the future, monomeric proteins with greater brightness and photostability will allow for even more intensive imaging experiments, efficiently folding monomeric photoconvertible proteins will improve our ability to perform photolabeling of fusion proteins, FRET pairs engineered to be orthogonal to the currently used CFP-YFP pairs will allow imaging of several biochemical activities in the same cell, and the long-wavelength end of the FP spectrum will continue to expand, allowing for more sensitive and efficient imaging in thick tissue and whole animals. By applying the principles put forth here, researchers may evaluate each new development in the field of FPs and make an informed decision as to whether it fits their needs.

Table 2 | Recommended filter sets

	Fluorescent protein	Excitation[a]	Emission[a]
Multiple labeling	Cerulean or CyPet	425/20	480/40
	mCitrine or YPet	495/10	525/20
	mOrange or mKO	545/10	575/25
	mCherry	585/20	675/130
	mPlum	585/20	675/130
Single labeling	T-Sapphire	400/40	525/80
	Cerulean or CyPet	425/20	505/80
	Emerald	470/20	530/60
	mCitrine or YPet	490/30	550/50
	mOrange or mKO	525/20	595/80
	tdTomato	535/20	615/100
	mStrawberry	550/20	630/100
	mCherry	560/20	640/100
	mPlum	565/40	670/120

[a]Values are given as center/bandpass (nm). Bandpass filters with the steepest possible cutoff are strongly preferred.

*Note: Supplementary information is available on the Nature Methods website.*

COMPETING INTERESTS STATEMENT
The authors declare competing financial interests (see *Nature Methods* website for details).

Published online at http://www.nature.com/naturemethods/
Reprints and permissions information is available online at http://npg.nature.com/reprintsandpermissions/

1. Nagai, T. *et al.* A variant of yellow fluorescent protein with fast and efficient maturation for cell-biological applications. *Nat. Biotechnol.* **20**, 87–90 (2002).
2. Nguyen, A.W. & Daugherty, P.S. Evolutionary optimization of fluorescent proteins for intracellular FRET. *Nat. Biotechnol.* **23**, 355–360 (2005).
3. Rizzo, M.A., Springer, G.H., Granada, B. & Piston, D.W. An improved cyan fluorescent protein variant useful for FRET. *Nat. Biotechnol.* **22**, 445–449 (2004).
4. Shaner, N.C. *et al.* Improved monomeric red, orange and yellow fluorescent proteins derived from Discosoma sp. red fluorescent protein. *Nat. Biotechnol.* **22**, 1567–1572 (2004).
5. Wang, L., Jackson, W.C., Steinbach, P.A. & Tsien, R.Y. Evolution of new nonantibody proteins via iterative somatic hypermutation. *Proc. Natl, Acad. Sci. USA* **101**, 16745–16749 (2004).
6. Zapata-Hommer, O. & Griesbeck, O. Efficiently folding and circularly permuted variants of the Sapphire mutant of GFP. *BMC Biotechnol.* **3**, 5 (2003).
7. Ando, R., Hama, H., Yamamoto-Hino, M., Mizuno, H. & Miyawaki, A. An optical marker based on the UV-induced green-to-red photoconversion of a fluorescent protein. *Proc. Natl. Acad. Sci. USA* **99**, 12651–12656 (2002).
8. Chudakov, D.M. *et al.* Photoswitchable cyan fluorescent protein for protein tracking. *Nat. Biotechnol.* **22**, 1435–1439 (2004).
9. Chudakov, D.M. *et al.* Kindling fluorescent proteins for precise *in vivo* photolabeling. *Nat. Biotechnol.* **21**, 191–194 (2003).
10. Karasawa, S., Araki, T., Nagai, T., Mizuno, H. & Miyawaki, A. Cyan-emitting and orange-emitting fluorescent proteins as a donor/acceptor pair for fluorescence resonance energy transfer. *Biochem. J.* **381**, 307–312 (2004).
11. Matz, M.V. *et al.* Fluorescent proteins from nonbioluminescent *Anthozoa* species. *Nat. Biotechnol.* **17**, 969–973 (1999).
12. Wiedenmann, J. *et al.* EosFP, a fluorescent marker protein with UV-inducible green-to-red fluorescence conversion. *Proc. Natl. Acad. Sci. USA* **101**, 15905–15910 (2004).
13. Verkhusha, V.V. & Sorkin, A. Conversion of the monomeric red fluorescent protein into a photoactivatable probe. *Chem. Biol.* **12**, 279–285 (2005).
14. Tsutsui, H., Karasawa, S., Shimizu, H., Nukina, N. & Miyawaki, A. Semi-rational engineering of a coral fluorescent protein into an efficient highlighter. *EMBO Rep.* **6**, 233–238 (2005).
15. Patterson, G.H. & Lippincott-Schwartz, J. Selective photolabeling of proteins using photoactivatable GFP. *Methods* **32**, 445–450 (2004).
16. Griesbeck, O., Baird, G.S., Campbell, R.E., Zacharias, D.A. & Tsien, R.Y. Reducing the environmental sensitivity of yellow fluorescent protein. Mechanism and applications. *J. Biol. Chem.* **276**, 29188–29194 (2001).
17. Zhang, J., Campbell, R.E., Ting, A.Y. & Tsien, R.Y. Creating new fluorescent probes for cell biology. *Nat. Rev. Mol. Cell Biol.* **3**, 906–918 (2002).
18. Tsien, R.Y. The green fluorescent protein. *Annu. Rev. Biochem.* **67**, 509–544 (1998).
19. Gross, L.A., Baird, G.S., Hoffman, R.C., Baldridge, K.K. & Tsien, R.Y. The structure of the chromophore within DsRed, a red fluorescent protein from coral. *Proc. Natl. Acad. Sci. USA* **97**, 11990–11995 (2000).
20. Hansen, M.C., Palmer, R.J., Jr, Udsen, C., White, D.C. & Molin, S. Assessment of GFP fluorescence in cells of *Streptococcus gordonii* under conditions of low pH and low oxygen concentration. *Microbiology* **147**, 1383–1391 (2001).
21. Zhang, C., Xing, X.H. & Lou, K. Rapid detection of a *gfp*-marked *Enterobacter aerogenes* under anaerobic conditions by aerobic fluorescence recovery. *FEMS Microbiol. Lett.* **249**, 211–218 (2005).
22. Verkhusha, V.V. & Lukyanov, K.A. The molecular properties and applications of *Anthozoa* fluorescent proteins and chromoproteins. *Nat. Biotechnol.* **22**, 289–296 (2004).
23. Zacharias, D.A., Violin, J.D., Newton, A.C. & Tsien, R.Y. Partitioning of lipid-modified monomeric GFPs into membrane microdomains of live cells. *Science* **296**, 913–916 (2002).
24. Long, J.Z., Lackan, C.S. & Hadjantonakis, A.K. Genetic and spectrally distinct *in vivo* imaging: embryonic stem cells and mice with widespread expression of a monomeric red fluorescent protein. *BMC Biotechnol.* **5**, 20 (2005).
25. Zhu, H. *et al.* Ubiquitous expression of mRFP1 in transgenic mice. *Genesis* **42**, 86–90 (2005).
26. Miesenböck, G., De Angelis, D.A. & Rothman, J.E. Visualizing secretion and synaptic transmission with pH-sensitive green fluorescent proteins. *Nature* **394**, 192–195 (1998).
27. Matsuyama, S., Llopis, J., Deveraux, Q.L., Tsien, R.Y. & Reed, J.C. Changes in intramitochondrial and cytosolic pH: early events that modulate caspase activation during apoptosis. *Nat. Cell Biol.* **2**, 318–325 (2000).
28. Hiraoka, Y., Shimi, T. & Haraguchi, T. Multispectral imaging fluorescence microscopy for living cells. *Cell Struct. Funct.* **27**, 367–374 (2002).
29. Habuchi, S. *et al.* Reversible single-molecule photoswitching in the GFP-like fluorescent protein Dronpa. *Proc. Natl. Acad. Sci. USA* **102**, 9511–9516 (2005).
30. Lukyanov, K.A., Chudakov, D.M., Lukyanov, S. & Verkhusha, V.V. Innovation: Photoactivatable fluorescent proteins. *Nat. Rev. Mol. Cell Biol.* (2005); advance online publication, 15 September 2005 (doi:10.1038/nrm1741).
31. Shkrob, M.A. *et al.* Far-red fluorescent proteins evolved from a blue chromoprotein from *Actinia equina*. *Biochem. J.* (2005); advance online publication, 15 September 2005 (doi: 10.1042/BJ20051314).

Supplementary Figure 1

A

B
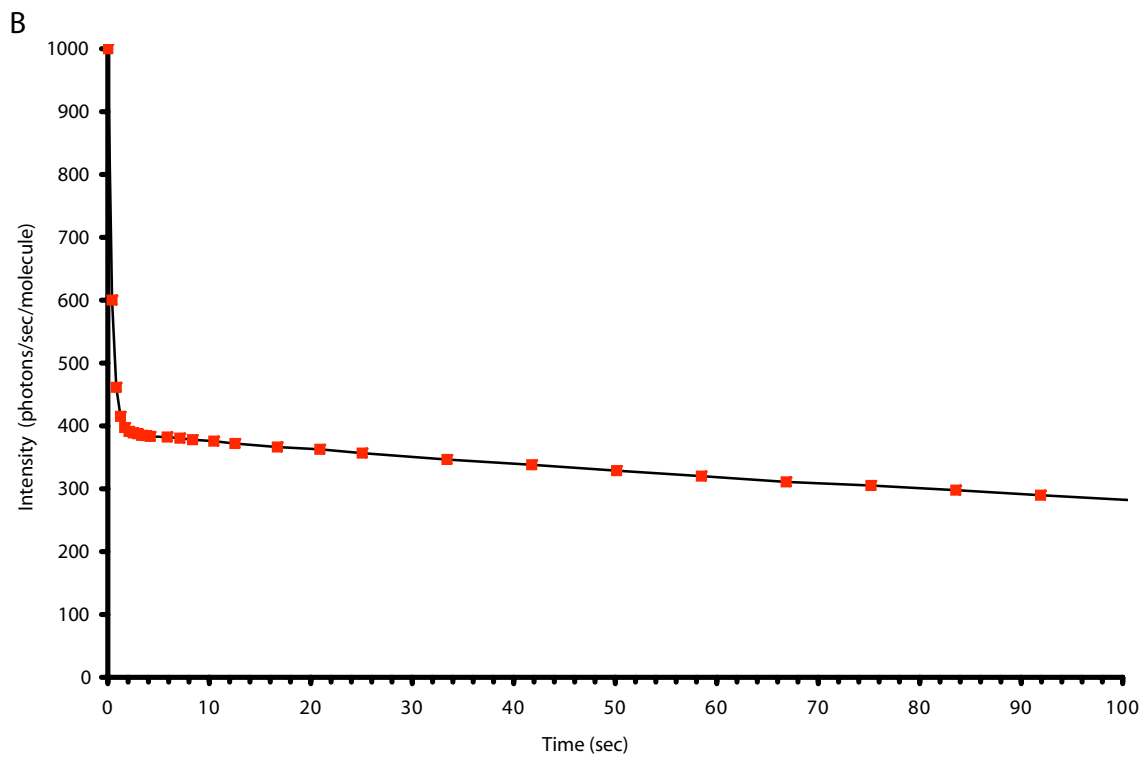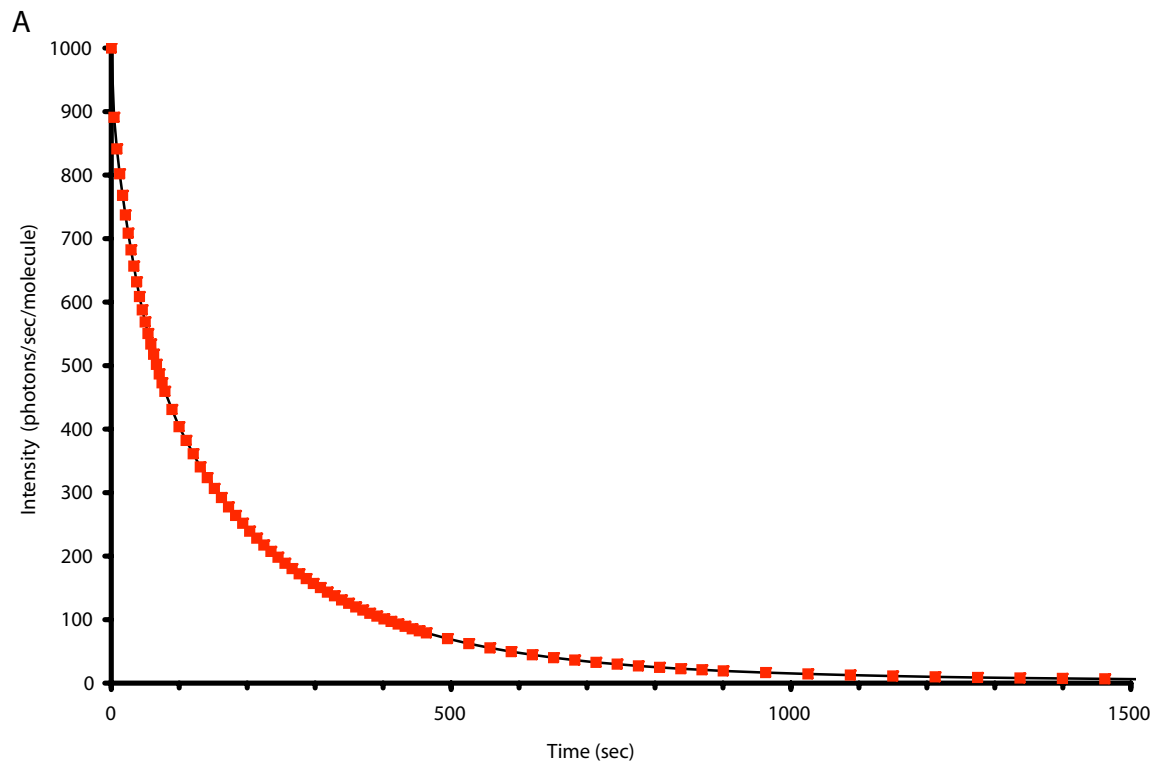
(A) mCherry photobleaching curve, showing nearly single exponential behavior
(B) Emerald photobleaching curve, showing pronounced fast initial component

Supplementary Table 1

Wavelength Class	Protein	Source Lab	Organism	Ex (nm)	Em (nm)	Extinction coefficient per chain, M⁻¹cm⁻¹	Fluorescence quantum yield	Brightness (EC*QY) (mM*cm)^-1	Brightness of fully mature protein (% of fluorescein)	$t_{0.5}$ for bleach, sec	photostability (fold improvement over fluorescein)	pKa	$t_{0.5}$ for maturation at 37°C	Oligomerization	References
Far-red	mPlum	Tsien	Discosoma sp.	590	649	41,000	0.10	4.1	5.9	53	7.3	<4.5	100 min	monomer	5
Red	mCherry	Tsien	Discosoma sp.	587	610	72,000	0.22	16	23	96	13.1	<4.5	15 min	monomer	4
	tdTomato	Tsien	Discosoma sp.	554	581	138,000	0.69	95	138	98	13.5	4.7	1 hr	tandem dimer	4
	mStrawberry	Tsien	Discosoma sp.	574	596	90,000	0.29	26	38	15	2.1	<4.5	50 min	monomer	4
	J-Red	Evrogen	Unidentified Anthomedusa	584	610	44,000	0.20	8.8	13	13	1.8	5	ND	dimer	x
	DsRed-Monomer	Clontech	Discosoma sp.	556	586	35,000	0.10	3.5	5.1	16	2.2	4.5	ND	monomer	y
Orange	mOrange	Tsien	Discosoma sp.	548	562	71,000	0.69	49	71	9.0	1.2	6.5	2.5 hr	monomer	4
	mKO	MBL Intl.	Fungia concinna	548	559	51,600	0.60	31	45	122	16.7	5	4.5 hr	monomer	10
Yellow	mCitrine	Tsien	Aequorea victoria	516	529	77,000	0.76	59	85	49	6.7	5.7	ND	monomer	16, 23
	Venus	Miyawaki	Aequorea victoria	515	528	92,200	0.57	53	76	15	2.0	6	ND	weak dimer	1
	YPet	Daugherty	Aequorea victoria	517	530	104,000	0.77	80	116	49	6.7	5.6	ND	weak dimer	2
	EYFP	Invitrogen	Aequorea victoria	514	527	83,400	0.61	51	74	60	8.3	6.9	ND	weak dimer	18
Green	Emerald	Invitrogen	Aequorea victoria	487	509	57,500	0.68	39	57	0.69	0.1	6	ND	weak dimer	18
	EGFP	Clontech*	Aequorea victoria	488	507	56,000	0.60	34	49	174	23.9	6	ND	weak dimer	y
Cyan	CyPet	Daugherty	Aequorea victoria	435	477	35,000	0.51	18	26	59	8.1	5	ND	weak dimer	2
	mCFP	Tsien	Aequorea victoria	433	475	32,500	0.40	13	19	64	8.8	4.7	ND	monomer	23
	Cerulean	Piston	Aequorea victoria	433	475	43,000	0.62	27	39	36	5.0	4.7	ND	weak dimer	3
UV-excitable green	T-Sapphire	Griesbeck	Aequorea victoria	399	511	44,000	0.60	26	38	25	3.5	4.9	ND	weak dimer	6
Reference	fluorescein pH 8.4			495	519	75,000	0.92	69	100	7.3	1.0	6.4			

* No longer commercially available
x www.evrogen.com
y www.clontech.com
ND = not determined

FPs not included in main table

Protein	Source	Comments
AceGFP	Evrogen	no clear advantage over well-validated Aequorea GFPs
AcGFP1	Clontech	no clear advantage over well-validated Aequorea GFPs
AmCyan1	Clontech	tetrameric
AQ143	Lukyanov	tetrameric
AsRed2	Clontech	tetrameric
Azami-Green/mAG	MBL Intl.	no clear advantage over well-validated Aequorea GFPs
cOFP	Stratagene	tetrameric
CopGFP	Evrogen	no clear advantage over well-validated Aequorea GFPs
dimer2, tdimer2(12)	Tsien	slower maturation than dTomato/tdTomato
DsRed/DsRed2/DsRed-Express	Clontech	tetrameric
EBFP	Clontech	Fast bleaching, dim, no longer commercially available
eqFP611	Weidenmann	poor folding at 37C, tetrameric
HcRed1	Clontech	dimeric, dim
HcRed-tandem	Evrogen	fast bleaching, dim
Kaede	MBL Intl.	dimmer and less efficient at photoconversion than KikGR
mBanana	Tsien	dim, fast photobleaching
mHoneydew	Tsien	dim, fast photobleaching
MiCy	MBL Intl.	dimeric, less spectral separation from YFPs than Aequorea GFP-derived CFPs
mRaspberry	Tsien	faster bleaching than mPlum
mRFP1	Tsien	dimmer and less photostable than mCherry
mTangerine	Tsien	fast bleaching, dimmer than mStrawberry
mYFP	Tsien	Chloride sensitivity
PhiYFP	Evrogen	suspected aggregation, faster bleaching than other YFPs, potential problems with fusion constructs
Renilla GFPs	various	dimeric, no clear advantages over well-validated Aequorea GFPs
TurboGFP	Evrogen	no clear advantage over well-validated Aequorea GFPs
ZsYellow1	Clontech	tetrameric

Supplementary Table 2

GFP variant	Mutations relative to wtGFP
EGFP [x,*]	F64L, S65T
Emerald [x]	F64L, S65T, S72A, N149K, M153T, I167T
EYFP [x,*]	S65G, V68L, S72A, T203Y
mYFP [x,*]	S65G, V68L, Q69K, S72A, T203Y, A206K
Citrine [x,*]	S65G, V68L, Q69M, S72A, T203Y
mCitrine [x,*]	S65G, V68L, Q69M, S72A, T203Y, A206K
Venus [*]	F46L, F64L, S65G, V68L, S72A, M153T, V163A, S175G, T203Y
YPet	F46L, I47L, F64L, S65G, S72A, M153T, V163A, S175G, T203Y, S208F, V224L, H231E, D234N
ECFP [x,*]	F64L, S65T, Y66W, N149I, M153T, V163A
mCFP [x,*]	F64L, S65T, Y66W, N149I, M153T, V163A, A206K
Cerulean [x,*]	F64L, S65T, Y66W, S72A, Y145A, H148D, N149I, M153T, V163A
CyPet	T9G, V11I, D19E, F64L, S65T, Y66W, A87V, N149I, M153T, V163A, I167A, E172T, L194I
EBFP [*]	F64L, S65T, Y66H, Y145F
T-Sapphire	Q69M, C70V, S72A, Y145F, V163A, S175G, T203I

[x] Some clones of *Aequorea* fluorescent proteins contain additional mutations believed to be neutral, such as K26R, Q80R, N146H, H231L, etc.variants

[*] Many GFP variants contain V inserted after Met1 so that the mRNA should contain an ideal translational start sequence. We number such a V as 1a to preserve wild-type numbering for the rest of the sequence.

Supplementary Table 3

Class	Protein	Source (Reference)	Ex (nm) [a]	Em (nm) [b]	EC [c]	QY [d]	Oligomerization	Comments
Photoactivatable								
	PA-GFP	Lippincott-Schwartz (15)	504	517	17,400	0.79	monomer (weak dimer)	Photoactivation with UV illumination
	Dronpa	MBL Intl. (29)	503	518	95,000	0.85	monomer	Reversible photoactivation with UV illumination
	PA-mRFP	Verkhusha (13)	578	605	10,000	0.08	monomer	Photoactivation with UV illumination
	KFP	Evrogen (9)	580	600	59,000	0.07	tetramer	Photoactivation with green light illumination
Photoconvertible								
	mEosFP	Wiedenmann (12)	505/569	516/581	67,200/37,000	0.64/0.62	monomer	Photoconversion from green to red with UV illumination
	tdEosFP	Wiedenmann (12)	505/570	516/582	84,000/33,000	0.66/0.60	tandem dimer	Photoconversion from green to red with UV illumination
	KikGR	MBL Intl. (14)	507/583	517/593	28,200/32,600	0.70/0.65	tetramer	Photoconversion from green to red with UV illumination
	PS-CFP2	Evrogen (8)	400/490	468/511	43,000/47,000	0.2/0.23	monomer	Photoconversion from cyan to green with UV illumination

[a,b,c,d] Before/after photoconversion

Supplementary Discussion

Measurement of time to bleach from 1000 down to 500 emitted photons/sec

In each bleaching experiment on the microscope, we measure the total excitation beam power exiting the microscope objective, with the sample replaced by a micro-integrating sphere attached to an ILC1700 meter (International Light, Newburyport MA), giving a detector current I in amperes. The manufacturer provides a NIST-traceable absolute calibration of this photodetector, $M( )$, in ampere/watt at 1 nm intervals. We know the relative output of a xenon lamp, $L( )$, in photons per 1 nm bandwidth, and we have separately measured the transmission of each excitation filter $F( )$ and dichroic mirror $D( )$. The energy of each photon of wavelength is $hc/\quad J( )$. The number of photons per nm at wavelength is given by $EL( )F( )D( )$, where the overall amplitude factor E is determined by the equation:

$$I = \int EL(\lambda)F(\lambda)D(\lambda)J(\lambda)M(\lambda)d\lambda \;\cong\; \sum_{400nm}^{700nm} EL(\lambda)F(\lambda)D(\lambda)J(\lambda)M(\lambda)\Delta\lambda$$

The rate of excitation X of each fluorophore is the integral of the respective contributions from photons of each wavelength interval. Each wavelength interval contributes $EL( )F( )D( )\;( )/A$, where $( )$ is the optical cross-section per molecule, and A is the area of illumination. $( )$ is proportional to the extinction coefficient $( )$ as follows: $( ) = (1000$ cm^3/liter)(ln 10) $( )/(6.023 \times 10^{23}$/mole$) = (3.82 \times 10^{-21}$ cm$^3 \cdot$M$) \cdot ( )$. Thus:

$$X = \int (E/A)L(\lambda)F(\lambda)D(\lambda)\sigma(\lambda)d\lambda \;\cong\; \sum_{400nm}^{700nm}(E/A)L(\lambda)F(\lambda)D(\lambda)\sigma(\lambda)\Delta\lambda$$

The initial rate of emission before any bleaching has occurred is simply XQ, where Q is the fluorescence quantum yield. Meanwhile the camera measures the relative intensity from the microscopic droplet as a function of time, from which the time t_{raw} to drop to 50% of the initial intensity can be readily measured by interpolation. We assume that reciprocity holds for XQ within an order of magnitude of 1000 photons/s, i.e. that bleaching time is inversely proportional to X. This reciprocity assumption has been verified for a few of the fluorescent proteins in Table 1, but is expected to break down when X is orders of magnitude greater than 1000 photons/s, i.e. under focused laser illumination. Assuming reciprocity:

t(to bleach 50% starting from 1000 photons/s) $= t_{raw}[XQ/(1000$ photons/s$)]$

We must admit that our numerical estimates of photobleaching have undergone some systematic revisions in successive publications, largely due to progressive recognition of the following errors. 1) It is more accurate to perform the above summations over wavelengths rather than to assume monochromaticity, i.e. to use just the meter calibration and extinction coefficient at the center of the excitation passband. 2) The mineral oil in which the microdroplets are suspended must be carefully pre-extracted to remove traces of acidic or quenching contaminants. 3) Many fluorescent proteins refuse to bleach with single exponentials or quantum yields and cannot be quantified as such. 4) Some fluorescent proteins have a very fast phase of partial bleaching that can be missed if one spends too much time focusing and setting up the measurement at too high an intensity. 5) Spatially nonuniform illumination can mean that the calibrated photodiode and the droplets imaged by the camera see different intensities.
Because of these uncertainties, the relative photostabilities reported within a single paper should be more reliable than the absolute values. However, the latter are still

important to enable comparison with other molecules and estimation of the feasibility of new experiments.